Cyclic deformation of bidisperse two-dimensional foams

M. Fátima Vaz,[1]*, S. J. Cox[2] and P. I. C. Teixeira[3,4]
[1] Instituto de Ciência e Engenharia de Materiais e Superfícies,
Instituto Superior Técnico, Universidade Técnica de Lisboa,
Avenida Rovisco Pais, P-1049-001 Lisboa, Portugal
[2] Institute of Mathematics and Physics, Aberystwyth University,
Ceredigion SY23 3BZ, United Kingdom
[3] Instituto Superior de Engenharia de Lisboa, Rua Conselheiro Emídio Navarro 1,
P-1950-062 Lisboa, Portugal
[4] Centro de Fisica Teórica e Computacional da Universidade de Lisboa,
Avenida Professor Gama Pinto 2, P-1649-003 Lisboa, Portugal

November 2, 2011

Abstract

In-plane deformation of foams was studied experimentally by subjecting bidisperse foams to cycles of traction and compression at a prescribed rate. Each foam contained bubbles of two sizes with given area ratio and one of three initial arrangements: sorted perpendicular to the axis of deformation (iso-strain), sorted parallel to the axis of deformation (iso-stress), or randomly mixed. Image analysis was used to measure the characteristics of the foams, including the number of edges separating small from large bubbles N_{sl}, the perimeter (surface energy), the distribution of the number of sides of the bubbles, and the topological disorder $\mu_2(N)$.

Foams that were initially mixed were found to remain mixed after the deformation. The response of sorted foams, however, depends on the initial geometry, including the area fraction of small bubbles and the total number of bubbles. For a given experiment we find that (i) the perimeter of a sorted foam varies little; (ii) each foam tends towards a mixed state, measured through the saturation of N_{sl}; and (iii) the topological disorder $\mu_2(N)$ increases up to an "equilibrium" value. The results of different experiments show that (i) the change in disorder, $\Delta\mu_2(N)$ decreases with the area fraction of small bubbles under iso-strain, but is independent of it under iso-stress; and (ii) $\Delta\mu_2(N)$ increases with ΔN_{sl} under iso-strain, but is again independent of it under iso-stress. We offer explanations for these effects in terms of elementary topological processes induced by the deformation that occur at the bubble scale.

Keywords: Two-dimensional foams, uniaxial deformation, segregation and mixing

1 Introduction

A liquid foam is an assembly of gas bubbles surrounded by liquid films. A bidisperse, or binary, foam consists of bubbles of only two sizes. The bubbles in a bidisperse foam may arrange in one of two possible kinds of configurations: (i) mixed, i.e., randomly dispersed, as usually occurs; and (ii) sorted, where there is segregation into regions containing only bubbles of one size. The important difference between mixed and segregated arrangements of bubbles can be seen in the fact that different regions of a foam will have different mechanical properties such as shear modulus. In granular materials, such a segregation is found frequently, and is well understood (the Brazil-nut effect), but has not been studied extensively in foams.

*Corresponding author - fatima.vaz@ist.utl.pt; fax: +351 218418132

A liquid foam tries to locally minimize its surface energy, which in two dimensions (2D) is proportional to the total perimeter. A further question then arises: to what extent can this local optimisation lead to a global optimisation? That is, given sufficient external stimulus, can the foam explore all possible sorted/segregated arrangements of the bubbles (a sort of ergodic hypothesis for foams) and find its energetic groundstate? The work reported here is a first step towards answering this question.

A study of the structure of static random bidisperse foams in 3D concluded that the fraction of larger bubbles and the ratio of bubble sizes were the two main factors that affected the (globally) optimal arrangement, in the sense of least energy (perimeter), of the foam [1]. Teixeira *et al.* [2] analysed whether sorted or mixed configurations of bubbles of two different sizes in 2D represent the global minimum energy state for bidisperse foams, given a bubble area ratio. Broadly speaking, if there is a large difference in the areas, bubbles tend to "mix", while if the areas are similar, the bubbles tend to "sort", i.e., segregate or assume phase-separated arrangements. Much greater complexity arises at intermediate area ratios, where the optimal state alternates between mixed and segregated.

An analogy can be made between bidisperse foams and the arrangement of solid objects. In fact, packings of discs or spheres are often used to study processes of mixing and sorting of biological cells and soap bubble arrangements. Several theoretical, experimental and numerical works on the assemblies or packing of two-size distribution of discs or spheres can be found in the literature [3, 4, 5, 6]. Some characteristics of the arrangements of random distribution of small and large discs, such as the number of edges separating small and large particles, N_{sl}, divided by the total number of edges N_t, were found to depend on the fraction of small bubbles and on the area ratio [4, 5, 6]. In a random bidisperse packing, N_{sl}/N_t attains a maximum value of 0.5 [6]. Values of N_{sl}/N_t smaller than 0.5 indicate phase separation or sorting of discs, as predicted by Richard *et al.* [5].

Foams, as well as granular media and emulsions, exhibit elastic-plastic behaviour when subjected to shear deformation, for example. The deformation or flow of foams is of extreme importance in industry, with applications in enhanced oil recovery, ore separation and personal care products, among many others. While the deformation of monodisperse or polydisperse foams has been studied extensively, there has been less work on the shear of bidisperse foams [7, 8, 9, 10]. In fact, bidisperse foams were found to behave differently to monodisperse foams when subjected to shear flow [7, 8, 9]. This difference in mechanical properties induced by the distribution of bubble sizes, and the relevance of foam flow to industry, makes this subject of particular importance.

Surface Evolver simulations of bidisperse foams under cyclic shear deformation [11] with fixed boundary conditions showed that the degree of mixing depended strongly on the liquid fraction and on the applied strain or extension: higher strains mean that more energy is pumped into the system, and high liquid fraction means that topological changes are triggered more easily. In both cases this leads to greater exploration of the energy landscape, suggesting that being mixed is the favoured state for the foam.

In this paper, we describe experiments on cyclic deformation of bidisperse foams. A cycle has two steps: one of traction and one of compression. Initially, the foam is subjected to traction, attains a maximum applied deformation, and is then compressed. One of the questions we address is whether a foam with initially well separated domains of large and small bubbles becomes mixed after being subjected to several deformation cycles. Another question is related to the evolution of an initially mixed configuration: are there conditions under which it will evolve to another arrangement or will it remain in the mixed configuration? (That is, what is the effective diffusion coefficient of the small bubbles, say, within the large ones?) In section 2 we describe the experimental procedure, and present our results in Section 3. These are discussed in Section 4, and we draw some conclusions in Section 5.

2 Experimental procedure

We denote by a_l the area of the large bubbles and a_s the area of the small bubbles. Each foam has n_s small bubbles and n_l large bubbles, giving a total of $n_t = n_s + n_l$ bubbles. The number fraction of small bubbles is the ratio $\nu_s = n_s/n_t$ and the area fraction of small bubbles is $x_s = n_s a_s/(n_s a_s + n_l a_l)$. Table 1 summarizes

Identifier	Number of cycles	Extension ϵ	Strain ratio R	Number of bubbles n_t	Number fraction of small bubbles ν_s	a_s (mm^2)	a_l (mm^2)	Area ratio a_l/a_s	Area fraction of small bubbles x_s
A1	20	0.72	0.010	259	0.72	3.16	13.05	4.13	0.38
A2	20	1.53	0.135	34	0.79	2.13	7.53	3.54	0.52
A3	20	1.27	0.143	64	0.70	1.56	7.24	4.64	0.34
A4	20	1.27	0.267	178	0.76	2.52	9.23	3.66	0.47
A5	20	1.45	0.096	147	0.67	2.51	9.13	3.64	0.36
B1	20	0.52	1.264	424	0.82	3.15	15.2	4.83	0.48
B2	20	1.84	0.511	35	0.51	2.46	9.5	3.86	0.22
B3	20	2.73	0.375	83	0.23	1.89	7.3	3.86	0.46
B4	20	0.51	0.296	255	0.68	2.37	9.02	3.81	0.36
C1	6	3.09	0.011	296	0.65	1.95	6.54	3.35	0.35
C2	6	1.61	0.310	223	0.65	1.68	9.55	5.68	0.25
C3	6	2.03	0.145	278	0.65	1.75	7.67	4.38	0.30

Table 1: Characteristics of the foams. Bubble areas are accurate to within 5%.

the geometrical properties of the different foams studied.

Foams were produced by the "liquid-glass" technique [12, 13, 14], in which bubbles are blown through a nozzle in a detergent solution. Two nozzles with different diameters were used to create small and large bubbles simultaneously, with a size dispersity of about 5% in each. The bubbles float to the surface and are trapped between the solution and a horizontal plexiglas plate, see Figure 1a. The gap width between the plate and the solution was around $g = 3$ mm in most of the experiments; small changes in g can be used to vary the effective liquid fraction.

Experiments were undertaken starting with three possible initial configurations of small/large bubbles as illustrated in Figure 2. Figures 2a and 2b show sorted distributions of bubbles in which large and small bubbles are separated by an interface almost parallel (type A) or perpendicular (type B) to the axis of deformation. Figure 2c shows a foam in which small and large bubbles are initially mixed (type C).

The foam is contained between two horizontal bars: one is fixed and the other moveable, to allow in-plane deformation of the foam. We denote by h the separation between the bars, as indicated in Figure 1a. In one cycle, the movable bar is displaced smoothly, parallel to the fixed bar, from the initial separation h_{imit} (see Figure 1b) up to a maximum separation, h_{max} (traction, see Figure 1c), returns past the initial state, h_{init} to a minimum separation h_{min} (compression, see figure 1d) and then back to h_{init} i.e. a fatigue test. h_{max} and h_{min} are not symmetrical relative to h_{init}; the applied extensional strain is defined as $\epsilon = (h_{max} - h_{min})/h_{min}$, and the strain ratio is $R = (h_{init} - h_{min})/(h_{max} - h_{init})$ (see Table 1).

Each cycle of traction and compression takes 60 seconds. Initially, experiments were performed with 6 cycles. While for type C foams, 6 cycles were enough to determine their behaviour, as the results were almost the same after 6 or 20 cycles, 6 cycles were too few to probe the dynamics of foams of types A and B. Therefore the experiments on those latter foams were continued to 20 cycles. No film ruptures were observed during the first 20 cycles, but after more than 20 cycles we found that bubbles started to break.

We chose to fix the deformation rate throughout. The maximum deformation is set by the size of the device and by the number of bubbles, since if a foam with a large number of bubbles is compressed to a small value of h, bubbles will escape from the device.

In order to assess the effect of deformation, we measured the number of edges that separate large from small bubbles, N_{sl}, normalized by total number of edges N_t, both as functions of time. The difference between the initial and final values of this measure of sorting is denoted by $\Delta(N_{sl}/N_t)$.

The image analysis software SigmaScan Pro 5 [15] allowed us to measure the liquid fraction as the area occupied by the liquid divided by the total foam area. We found values of between 3% and 9%. The foam was then skeletonized, and the total perimeter P, equivalent to the surface energy in units of the film

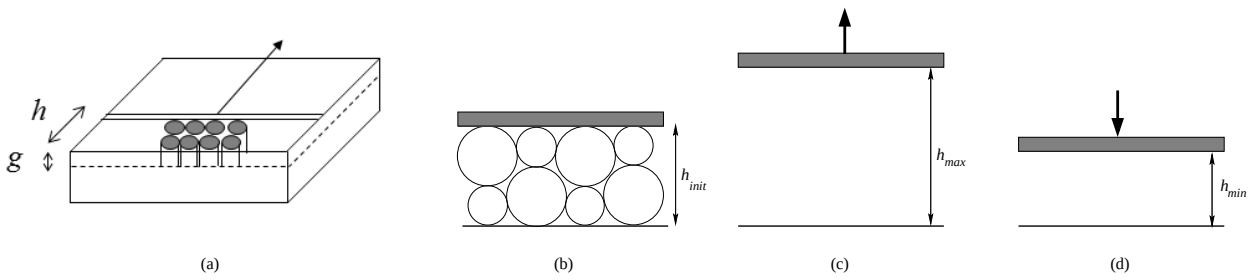

Figure 1: Sketch of the in-plane deformation of a bidisperse foam. (a) The foam consists of a single layer of bubbles sandwiched between a pool of liquid at the bottom and a plexiglas plate on top. The layer thickness is the width of the gap between liquid and plate, g. The foam is bounded laterally by two bars, one fixed and one moveable, a (variable) distance h apart; this allows extensional strains to be applied in the plane of the foam. (b) Top view of the initial stage: the separation between bars is h_{init}; (c) top view of foam under maximum traction; and (d) top view of foam under maximum compression. The arrows indicate the axis of deformation.

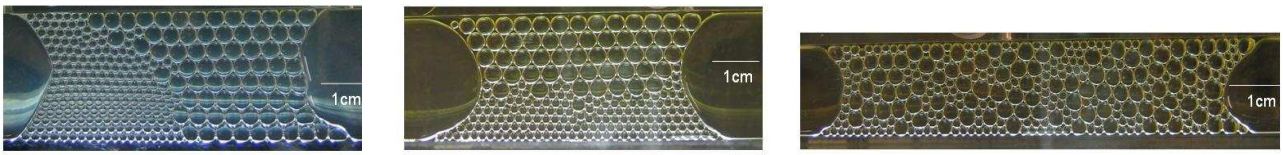

Figure 2: Photographs, taken from above, illustrating the three initial distributions of bidisperse 2D foams: (a) large and small bubbles are initially separated by an interface almost parallel to the axis of deformation (type A); (b) large and small bubbles are initially separated by an interface almost perpendicular to the axis of deformation (type B); (c) large and small bubbles are initially mixed (type C).

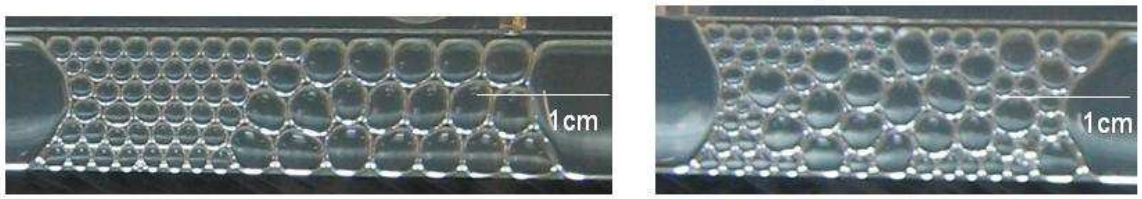

(a) (b)

Figure 3: Initial (a) and final (b) configurations of foam A3, after 20 cycles.

tension γ, of the resulting dry foam was measured. Note that γ is not measured, and indeed not required to understand the change in the topology of the foam. In order to be able to compare different foams, we scale the perimeter by the total area of the foam to give what we shall refer to as the "normalized perimeter":

$$\hat{P} = \frac{P}{\sqrt{n_s a_s + n_l a_l}}. \tag{1}$$

Distribution functions for the number of neighbours surrounding each bubble were determined both before and after the deformation. The topological disorder of the number of neighbours was evaluated from the second moment of the distribution $\mu_2(N) = \Sigma p(N)(N - \langle N \rangle)^2$, where $p(N)$ is the fraction of bubbles with N sides, and the difference between the initial and final values, $\Delta\mu_2(N)$, was calculated.

3 Results

Figure 3 shows photographs of a foam of type A, before and after 20 cycles of deformation. Even after 20 cycles of deformation, some areas of the foam remain size segregated (sorted). Nonetheless, it would appear that the foam has started to mix.

Figure 4 presents the evolution of the fraction of edges separating large from small bubbles N_{sl}/N_t as a function of the number of cycles, for several experiments of type A, B and C. Note that in the case of foams of type C, N_{sl}/N_t remains almost constant throughout the experiment, so we performed only 6 cycles in each of the three runs. For foams of types A and B, the value of N_{sl}/N_t increases towards one half, indicating a transition from sorted to mixed arrangements as anticipated in the photographs of Figure 3.

In Figure 5, the evolution of N_{sl}/N_t in a single experiment of type A (the result is similar for a foam of type B) is compared with the corresponding values of the normalized perimeter $\hat{P}$ and disorder $\mu_2(N)$. The perimeter changes little with repeated deformation, although it does oscillate during each cycle due to film stretching followed by topological changes, while $\mu_2(N)$ increases in much the same way as N_{sl}/N_t, indicating that the disorder appears to offer another measure of the degree of mixing. The error associated with the normalized perimeter is around 6%.

Figure 6 presents the distribution of the number of sides of small and large bubbles, n, both before and after 20 cycles of deformation, for foams of types A and B. To emphasise the shift in the distribution of large bubbles to higher n, data from four experiments were averaged.

4 Discussion

In the present paper, the effect of a dynamic deformation – the application of traction/compression cycles – on the structure of a bidisperse two-dimensional foam was studied. To characterise the foams and the degree of mixing/sorting, we measured the number of edges separating small from large bubbles, the perimeter (surface energy), the topological disorder and the number of sides of a bubble.

For initially mixed foams, type C, there is no dependence of these measures on the number of cycles, for example N_{sl}/N_t remains constant around 0.5 (see Figure 4c). As a result, a mixed arrangement keeps its mixed character and does not evolve towards another type of configuration.

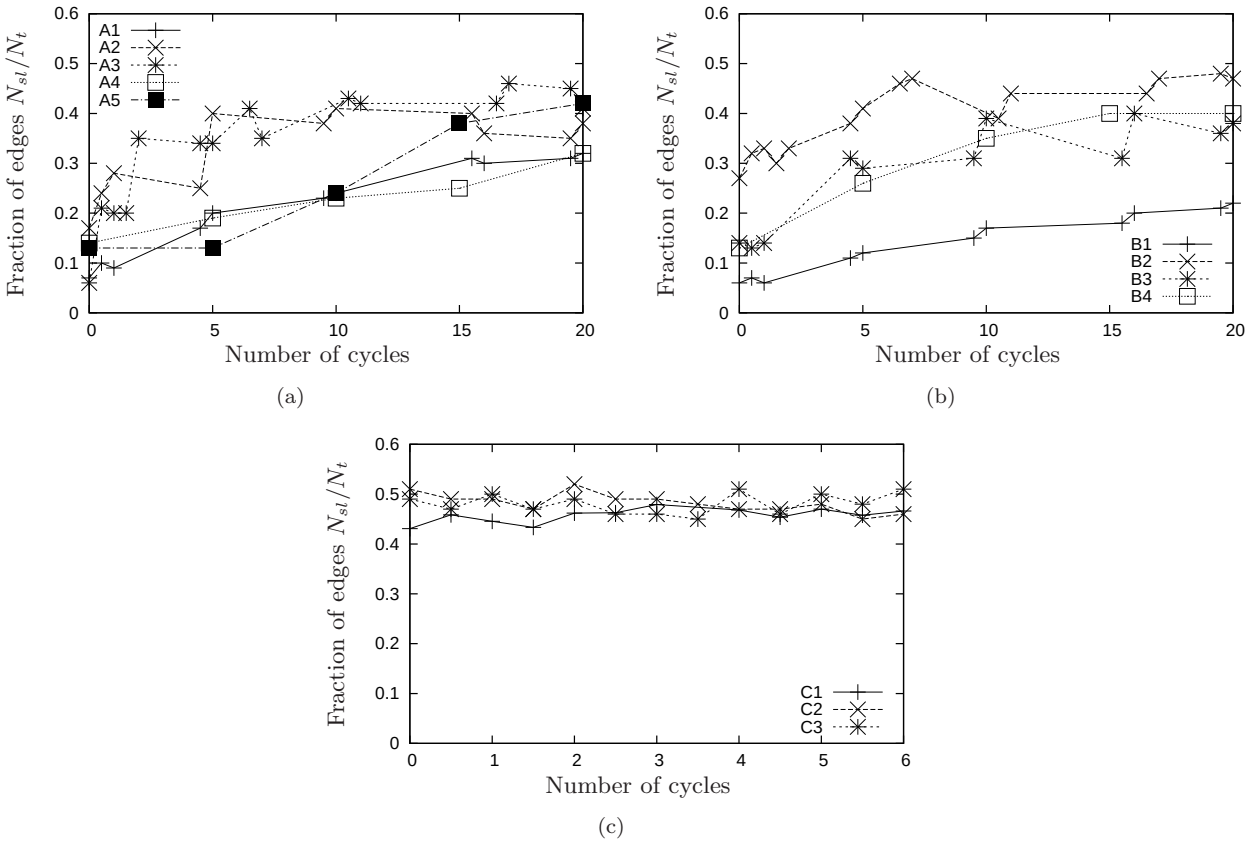

Figure 4: Fraction of edges separating large from small bubbles, N_{sl}/N_t for different bidisperse foams with an initial distribution of cells of type A (a), type B (b) and type C (c), as a function of the number of cycles.

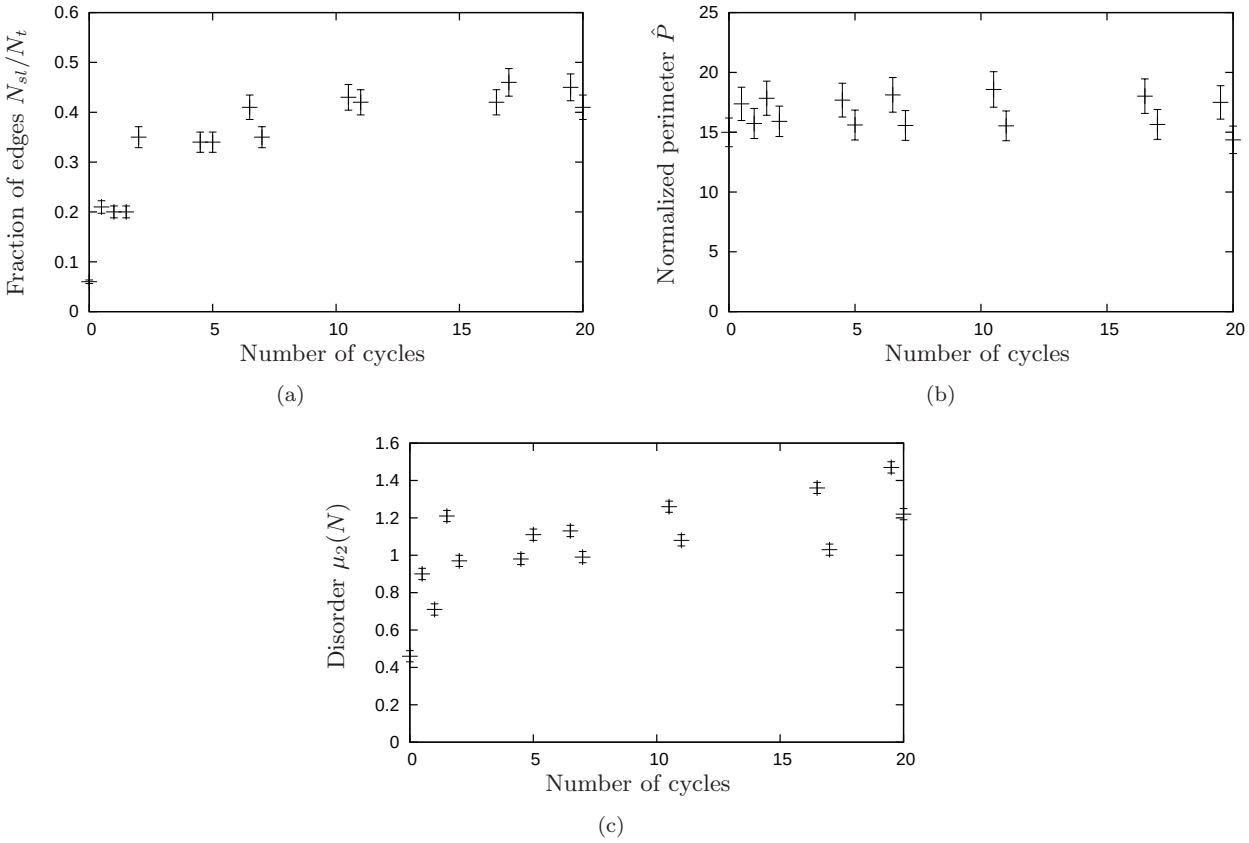

Figure 5: Evolution of foam A3 during an experiment of 20 cycles: (a) fraction of edges N_{sl}/N_t (from figure 4); (b) normalized perimeter $\hat{P}$; and (c) disorder, $\mu_2(N)$.

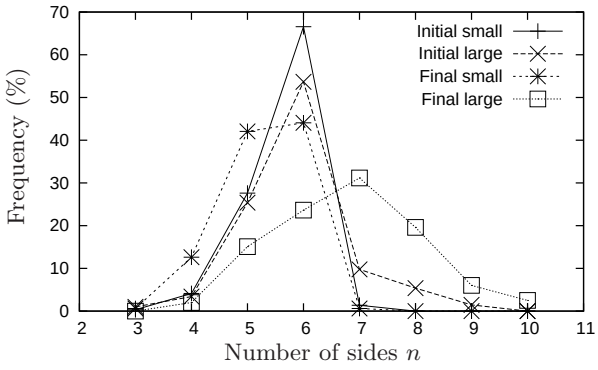

Figure 6: Shift in the distribution of the number of sides of small and large bubbles, comparing the initial distribution with that after 20 cycles. The data are obtained from an average over four experiments: A2, A3, B2 and B3.

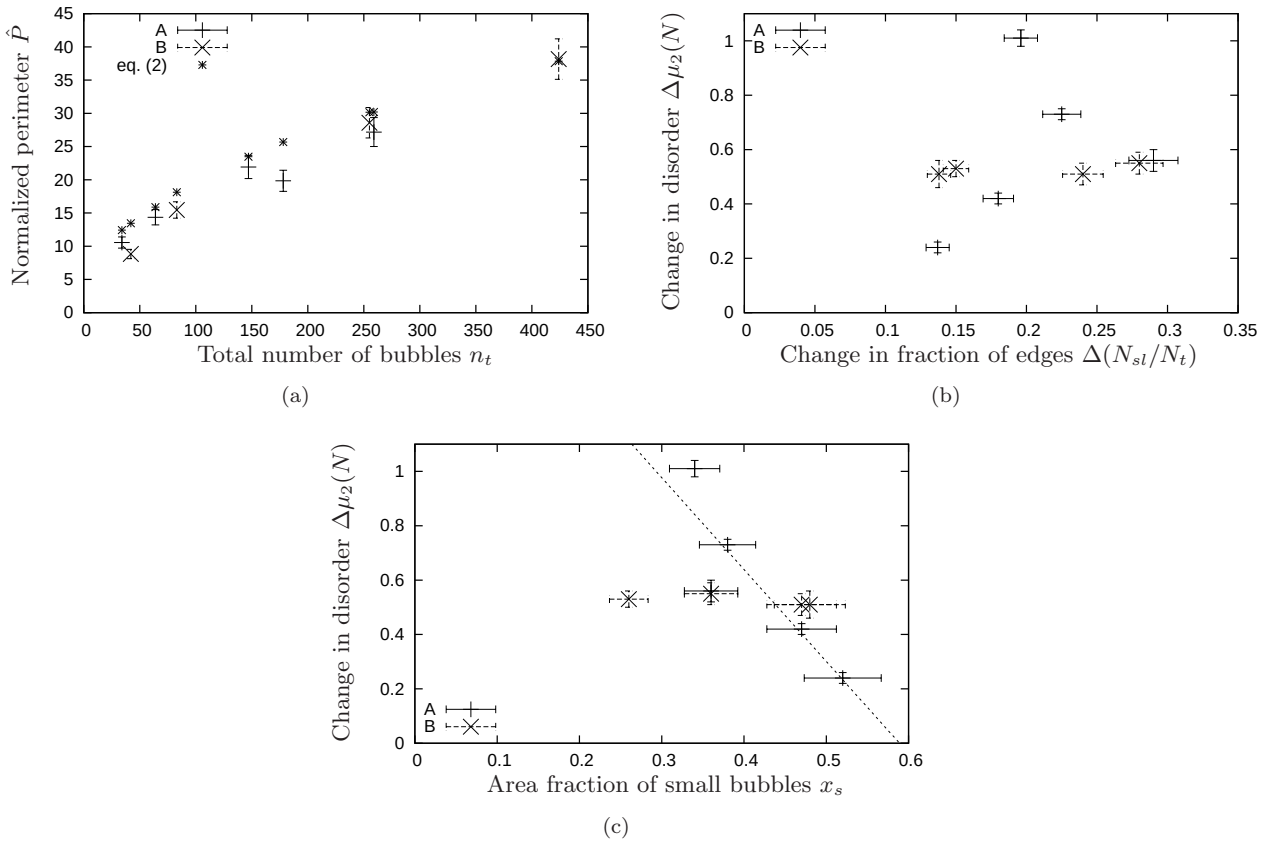

Figure 7: (a) The measured and estimated normalized perimeter $\hat{P}$ at the end of an experiment as a function of the total number of bubbles, n_t, has approximately square-root behaviour; instead we make a direct comparison with eq. (2), which is seen to capture the same effect but slightly overestimates the experimental data. (b) The change in disorder $\Delta\mu_2(N)$ increases with the change in the fraction of edges between small and large bubbles for foams of type A, but is independent of this fraction for foams of type B. (c) The change in disorder $\Delta\mu_2(N)$ decreases with the area fraction of small bubbles x_s for foams of type A – the line shown is a linear fit to this data – but is independent of this fraction for foams of type B. In all cases error bars were estimated by performing three independent measurements of each quantity.

In foams of type A and of type B, an initially sorted foam evolves towards a mixed arrangement. The evolution observed here is by no means complete: there remain regions with only small or large bubbles. Nonetheless, N_{sl}/N_t increases with the number of cycles and in some cases it reaches values close to 0.5, which is expected for a mixed foam [6], as in experiments of type C. We believe that the theoretical value would be attained under ideal conditions: an infinite number of cycles and no film rupture.

The normalized perimeter was examined to assess if the deformation induced a motion towards the energetic groundstate. As can be seen in Figure 5b), within a single experiment $\hat{P}$ fluctuates around a constant value, being slightly higher in traction than in compression. Although the arrangement tends to a mixed state (Figure 4b), the change in the perimeter of the system remains smaller than the fluctuations, indicating that $\hat{P}$ depends mainly on the total number of bubbles, as shown in Figure 7a), rather than the details of the arrangement, and is only slightly over-estimated by the formula of Vaz *et al.* [16]:

$$\hat{P} = \frac{3.72}{2} \frac{\Sigma_i a_i^{1/2}}{(\Sigma_i a_i)^{1/2}} + 2.04. \tag{2}$$

That is, $\hat{P}$ should increase with the square-root of the number of bubbles. Note that this equation was

derived for a circular foam, which is not the case here, so the last term should be somewhat higher than 2.04.

The number of sides of each bubble of the foam was measured. Since no differences were found in the side distribution functions of type A compared to type B foams (data not shown) we show an average over four experiments in Figure 6. At the beginning of the experiments, the distribution functions of the large and small bubbles are not clearly distinct. However, by the end of experiments the distributions are separated, with large bubbles now having a larger number of sides. A smaller effect, a decrease in the number of sides, is also apparent for small bubbles. Thus at the end of the deformation, larger bubbles will be surrounded by a larger number of sides, while small bubbles will have a lower number of sides, moving the structure into line with the qualitative predictions of Lewis and Feltham (see [17] and references therein).

In any given experiment, the topological disorder of the number of sides, which was evaluated by the second moment of the distribution, $\mu_2(N)$, increases initially but appears to reach a plateau (Figure 5c), just as it does during the diffusion-driven coarsening of an initially ordered bubble structure [18]. The evolution of the topological disorder of a bidisperse foam, under cyclic shear deformation, was also similar [8]. This suggests that our foams may have reached an asymptotic regime, which we have yet to characterize fully.

In order to make comparisons between different experiments, it is necessary to measure the change in our two measures of mixing, $\Delta(N_{sl}/N_t)$ and $\Delta\mu_2(N)$. In figure 7b) we see a striking difference between foams of types A and B: in the former case, the change in disorder varies widely with $\Delta(N_{sl}/N_t)$, while in the latter case the two are independent. We attribute this to the fact that the deformation of a type A foam can be viewed as an iso-strain experiment, in which both halves of the foam are subjected to the same strain but respond in different ways due to the difference in bubble size (leading to different stiffnesses). On the other hand, the deformation of a foam of type B is an iso-stress experiment, since despite the differences in bubble size both halves of the foam must experience the same stress. This means that the development of a more mixed state in the iso-strain case (type A) is accompanied by a large change in disorder, while in the case of iso-stress (type B) the change in disorder is constant and is not a good measure of the degree of mixing.

Of all the geometrical parameters that describe an arrangement of bubbles, the area fraction of small bubbles appears to play a fundamental role: for foams of type A the change in disorder decreases as the area fraction of small bubbles, x_s, increases (see Figure 7c; the rms error in the fit is 0.158). Thus, an arrangement with small x_s, will have a large change in disorder. This dependence on area fraction is in agreement with earlier work [1, 2, 5, 6]; note the contrast with foams of type B, and with static conditions, for which the arrangement of bidisperse bubbles or discs depends mainly on the *number* fraction of small bubbles (a fit of our data to number fraction has an rms error of 0.246).

Previously, simulations with fixed rectangular boundary conditions and liquid fractions up to about 3% [11] suggested that high liquid fractions and high strains promote mixing. Our experiments showed no effect on the degree of mixing as liquid fraction varied (in the range 6 to 9%), or strain increased. We speculate that with weaker constraints on the motion of the foam (i.e., not completely confining the foam), high strain is insufficient to trigger mixing; moreover, a moderate liquid fraction appears to be required, but provided it is above a certain threshold, its value is not important.

5 Conclusions

The effect of uniaxial deformation on the mixed and sorted characteristics of bidisperse foams was assessed. Several foam arrangements with different properties were studied. Although various parameters may be used to characterize a foam configuration, the geometrical parameter that controlled the deformation process was found to be the area fraction of small bubbles.

Arrangements of random mixed foams remain mixed after a few cycles of traction/compression. Initially sorted arrangements become increasingly mixed with deformation, measured by either an increase in the number of edges between small and large bubbles or by an increase in the topological disorder. The final arrangement of the foam consists of large bubbles surrounded by an above average number of bubbles, while small bubbles have fewer neighbours than average. It seems that initially sorted configurations of bubbles

tend to achieve an "equilibrium" or steady state, characterized by a constant value of the second moment of the distribution of sides.

In the future, it would be instructive to exactly reproduce a given arrangement and vary the parameters more widely. Experiments of the type described here could also be performed at higher deformation rate, to test the effect of rate on mixing. Finally, to determine the relation between local and global energy optimization, more theoretical work is required to find the groundstate configurations of a bidisperse foam cluster as a function of area fraction and area ratio.

Acknowledgements

MFV thanks F. Thomas, C. Quillet and F. Graner, from the Laboratoire de Spectrométrie Physique, Université de Grenoble, who made possible the performance of the initial experiments. We also thank F. Graner for useful comments on an earlier draft. The work was carried out under the Anglo-Portuguese Joint Research Programme, Treaty of Windsor, Project B/U20, 2010. SJC also acknowledges financial support from EPSRC EP/D071127/1.

References

[1] A. M. Kraynik, D. A. Reinelt, F. van Swol, Structure of random bidisperse foam, Colloids and Surfaces A: Physicochem. Eng. Aspects 263 (2005) 11–17.

[2] P. I. C. Teixeira, F. Graner, M. A. Fortes, Mixing and sorting of bidisperse two-dimensional bubbles, Eur. Phys. J E, 9 (2002) 161–169.

[3] C. N. Likos, C. L. Henkley, Complex alloy phases for binary hard-disc mixtures, Phil. Mag. B 68 (1993) 85–113.

[4] C. Annic, J. P. Troadec, A. Gervois, J. Lemaitre, M. Ammi, L. Oger, Experimental Study Of Radical Tesselations Of Assemblies Of Disks With Size Distribution, J. Phys. I France 4 (1994) 115–125.

[5] P. Richard, L. Oger, J. P. Troadec, A. Gervois, Tesselation of binary assemblies of spheres, Physica A 259 (1998) 205–221.

[6] P. Richard, L. Oger, J. P. Troadec, A. Gervois, A model of binary assemblies of spheres, Eur. Phys. J. E 6 (2001) 295–303.

[7] G. Katgert, M. E. Mobius, M. van Hecke, Rate Dependence and Role of Disorder in Linearly Sheared Two-Dimensional Foams, Phys. Rev. Lett., 101 (2008) 05831.

[8] C. Quilliet, S. A. Talebi, D. Rabaud, J. Kafer, S. J. Cox, F. Graner, Topological and geometrical disorders correlate robustly in two-dimensional foams, Philosophical Magazine Letters, 88 (2008) 651–660.

[9] G. Katgert, A. Latka, M. E. Mobius, M. van Hecke, Flow in linearly sheared two dimensional foams: from bubble to bulk scale, Phys. Rev. E 79 (2009) 066318.

[10] G. Katgert, M. van Hecke, Jamming and Geometry of Two-Dimensional Foams, EPL, 92 (2010) 34002.

[11] S. J. Cox, The mixing of bubbles in two-dimensional bidisperse foams under extensional shear, J. Non-Newtonian Fluid Mech. 137 (2006) 39–45.

[12] M. F. Vaz, M. A. Fortes, Experiments on defect spreading in hexagonal foams, J. Phys. Condens. Matter, 9 (1997) 8921–8935.

[13] M. F. Vaz, S. J. Cox, Two-bubble instabilities in quasi-two-dimensional foams, Phil. Mag. Letts. 85 (2005) 415–425.

[14] B. Dollet, F. Graner, Two-dimensional flow of foam around a circular obstacle: local measurements of elasticity, plasticity and flow, J. Fluid Mech., 585 (2007) 181–211.

[15] Sigma Scan software. www.systat.com.

[16] M. F. Vaz, M. A. Fortes, F. Graner, Surface energy of free clusters of bubbles: an estimation, Phil. Mag. Lett., 82 (2002) 575–579.

[17] M.A. Fortes, P.I.C. Teixeira, Bubble size-topology correlations in two-dimensional foams derived from surface energy minimization, J. Phys. A: Math. Gen., 36 (2003) 5161–5173.

[18] J. Stavans, J. A. Glazier, Soap froth revisited: dynamic scaling in the two-dimensional froth, Phys. Rev. Lett., 62 (1989) 1318–1321.